Taylor & Francis
Taylor & Francis Group

Natural Product Research
Formerly Natural Product Letters

ISSN: (Print) (Online) Journal homepage: https://www.tandfonline.com/loi/gnpl20

New lanostane-type triterpenoids with proangiogenic activity from the fruiting body of *Ganoderma applanatum*

Chunjiao Jiang, Jiancheng Ji, Peihai Li, Wenfeng Liu, Hao Yu, Xiuqing Yang, Lili Xu, Lizhong Guo & Yaqin Fan

To cite this article: Chunjiao Jiang, Jiancheng Ji, Peihai Li, Wenfeng Liu, Hao Yu, Xiuqing Yang, Lili Xu, Lizhong Guo & Yaqin Fan (2021): New lanostane-type triterpenoids with proangiogenic activity from the fruiting body of *Ganoderma applanatum*, Natural Product Research, DOI: 10.1080/14786419.2021.1898388

To link to this article: https://doi.org/10.1080/14786419.2021.1898388

NATURAL PRODUCT RESEARCH
https://doi.org/10.1080/14786419.2021.1898388

New lanostane-type triterpenoids with proangiogenic activity from the fruiting body of *Ganoderma applanatum*

Chunjiao Jiang[a]*, Jiancheng Ji[a]*, Peihai Li[b], Wenfeng Liu[c], Hao Yu[a], Xiuqing Yang[a], Lili Xu[a], Lizhong Guo[a] and Yaqin Fan[a,c]

[a]Shandong Provincial Key Laboratory of Applied Mycology, College of Life Sciences, Qingdao Agricultural University, Qingdao, China; [b]Biology Institute, Qilu University of Technology (Shandong Academy of Sciences), Jinan, China; [c]Key Laboratory of Science and Technology for Marine Ecology and Environment, First Institute of Oceanography, Ministry of Natural Resources, Qingdao, China

ABSTRACT

Two new lanostane-type triterpenoids, ganoderenicfys A (**1**) and B (**2**), together with six related known terpenoids (**3**–**8**), were isolated and identified from the fruiting body of *Ganoderma applanatum*. The structures of these compounds were established on the basis of detailed interpretation of their NMR and HRESIMS data. The absolute configurations of **1** and **2** were determined by quantum chemical electronic circular dichroism (ECD) calculations. All of the isolated compounds were evaluated for their proangiogenic activities in a transgenic fluorescent zebrafish model. Compounds **1**–**6** displayed dose-dependently proangiogenic activity in a PTK787-induced vascular injury zebrafish model, while compounds **1**, **2** and **4** significantly promoted the angiogenesis. This is the first report for proangiogenic activities of lanostane-type triterpenoids.

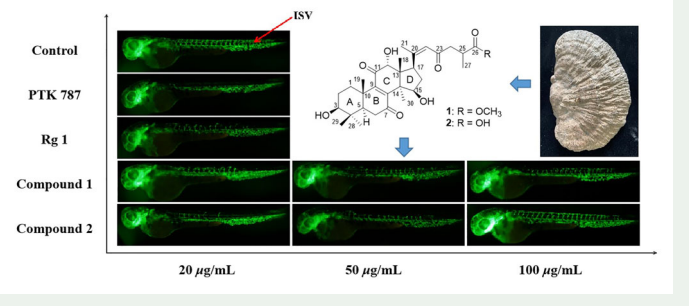

ARTICLE HISTORY
Received 5 November 2020
Accepted 28 February 2021

KEYWORDS
Lanostane-type triterpenoids; *Ganoderma applanatum*; proangiogenic activity

1. Introduction

Angiocardiopathy (cardiovascular disease, CVD) is one of the deadliest diseases, causing more than 17 million deaths worldwide each year (Benjamin et al. 2019).

CONTACT Yaqin Fan fanyaqin@qau.edu.cn
*Chunjiao Jiang and Jiancheng Ji contributed equally to this work.

Supplemental data for this article can be accessed at https://doi.org/10.1080/14786419.2021.1898388.

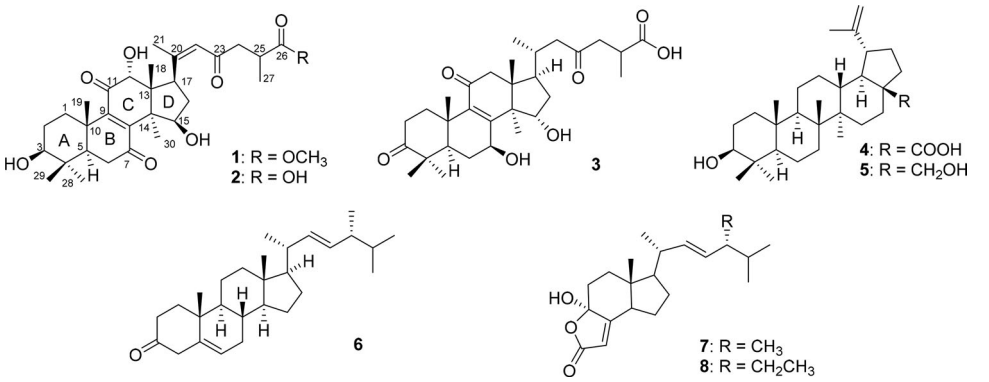

Figure 1. Structures of compounds **1**–**8** isolated from *Ganoderma applanatum*.

Insufficient angiogenesis is the most common cause of ischaemic CVDs, including ischaemic heart disease, peripheral arterial disease, and stroke (Kurusamy et al. 2017). Pro-angiogenesis refers to promoting or inducing ischemic tissues to form new vascular network, or sprout new blood vessels on original blood vessels through various means. As the result, the body can realize blood supply reconstruction, improve blood supply insufficiency, and achieve the therapeutic effect of CVDs (Carmeliet and Jain 2011). In recent years, pro-angiogenesis has been highly valued as a new target for the development of cardiovascular drugs (Gut et al. 2017).

Natural products have historically been a rich source of new drugs or drug candidates. *Ganoderma*, a group of wood degrading basidiomycete mushroom with hard fruiting bodies, is a famous medicinal plant which has long been regarded as one of the most significant medicinal mushrooms worldwide (Isaka et al. 2017). The medicinal effects of *Ganoderma* have prompted a wide range of studies on its active ingredients, including terpenoids, alkaloids, fatty acids, polysaccharides, nucleotides, and so on (Zhang et al. 2019). Some of these metabolites exhibited intriguing biological properties (Luo et al. 2019), such as antitumor (Weng et al. 2010; Qin et al. 2020), anti-inflammatory (Tung et al. 2013), hepatoprotective properties (Gao et al. 2018), neuroprotective (Zhou et al. 2015) and antioxidant (Sun et al. 2004). Furthermore, the metabolites of *Ganoderma* have also received considerable attention due to their potential clinical effects on CVD, which could prevent from heart damage in a variety of disease models (Meng and Yang 2019).

In order to search for proangiogenic bioactive constituents from *G. applanatum*, a systematic phytochemical study was performed. As a result, two previously undescribed lanostane-type triterpenoids, ganoderenicfys A (**1**) and B (**2**), together with six related known terpenoids, ganoderic acid A (**3**) (Seo et al. 2009), betulinic acid (**4**), betulin (**5**) (Chatterjee et al. 1999), (22E)-ergosta-5,22-dien-3-one (**6**) (Xu et al. 2018), demethylincisterol A4 (**7**), and demethylincisterol A3 (**8**) (Mansoor et al. 2005) (Figure 1), were isolated and identified from the fruiting body of *G. applanatum*. Compounds **1**–**6** showed different levels of proangiogenic activities on zebrafish. Compounds **1**, **2**, and **4** significantly promoted the angiogenesis in a dose-dependent manner. Herein, the isolation, structural elucidation, and bioactivity of these compounds were reported.

2. Results and discussion

Ganoderenicfy A (**1**) was obtained as white amorphous powder. The molecular formula was $C_{31}H_{44}O_8$ on the basis of a HRESIMS (Figure S1) peak at m/z 545.3113 $[M+H]^+$ and NMR data (Table S1, Figures S2 and S3), indicating 10 degrees of unsaturation. The ^{1}H NMR spectrum of **1** showed the presence of eight methyl proton signals (including six singlets, one doublet, and one oxygenated singlet), three oxymethines, and a singlet olefinic proton. The ^{13}C-DEPTQ-NMR (Table S1, Figure S3) and HSQC (Figure S4) spectra revealed the presence of 31 carbon atoms, which were clarified into eight methyls (including one methoxy group), five methylenes, seven methines (including three oxygenated and one olefinic), and eleven quaternary carbons (including three olefinic and four carbonyls). The above data were very similar to those of elfvingic acid A (Yoshikawa et al. 2002) except for the absence of C-3 ketone signal at δ_C 215.2 and the presence of signals for an additional oxymethine at $\delta_{C/H}$ 75.5/3.08 (CH-3) and a methoxy group at $\delta_{C/H}$ 51.5/3.57 (OCH_3). The key ^{1}H-^{1}H COSY (Figures S5 S16) correlations of H_2-1 (δ_{H2} 1.17, 2.67)/H_2-2 (δ_H 1.56)/H-3, together with HMBC (Figures S6 and S16) correlations from H_3-28 (δ_H 0.92) to the oxymethine C-3 and H-3 to C-2 (δ_C 27.3) and C-28 (δ_C 27.8), suggested that compound **1** bears a hydroxyl rather than a ketone as in elfvingic acid A at C-3. The location of the methoxy group at C-26 was demonstrated by HMBC correlation from the methoxy protons (δ_H 3.57) to C-26 (δ_C 175.7). The overall planar structure of **1** was finally defined by the HMBC and COSY correlations as shown in Figure S16.

The relative configuration of **1** was assigned by analysis of the NOESY data (Figure S7 and S17). NOE correlations from H-6β (δ_H 2.64) to H_3-19 (δ_H 1.23) and H_3-29, and from H_3-18 (δ_H 0.76) to H-12 (δ_H 3.58), H_3-19 and H_3-21 (δ_H 2.09) indicated the cofacial orientation of these protons, and the correlations from H-5 (δ_H 1.51) to H-3 and H_3-28 (δ_H 0.92), from H-6α (δ_H 2.34) to H_3-28, and from H_3-30 (δ_H 1.28) to H-15 (δ_H 4.25) and H-17 (δ_H 3.15) suggested that these groups are on the face opposite to H_3-19. In order to assign the absolute configuration of **1**, conformational analysis and TDDFT-ECD calculations were performed on the arbitrarily chosen of (3*S*, 5*R*, 10*S*, 12*R*, 13*R*, 14*R*, 15*R*, 17*R*)-**1**. The TDDFT-ECD spectra of the optimized MMFF conformers were calculated at the BH&HLYP/TZVP and CAM-B3LYP/TZVP levels. The computed ECD spectra of (3*S*,5*R*,10*S*,12*R*,13*R*,14*R*,15*R*,17*R*)-**1** matched well to the experimental ECD spectrum, which showed positive cotton effects (CEs) near 220 and 275 nm and negative CE near 245 nm (Figure S18).

Ganoderenicfy B (**2**) was isolated as white amorphous powder. The molecular formula of **2** was assigned as $C_{30}H_{42}O_8$ based on its HRESIMS (Figure S8) ion peak at *m/z* 531.2968 $[M+H]^+$ (calcd for $C_{30}H_{43}O_8$, 531.2952). Interpretation of the ^{1}H and ^{13}C NMR, as well as HSQC data (Table S1, Figures S9–S12), of compound **2** indicated the presence of 30 carbons, which were clarified into seven methyls, five methylenes, seven methines (three oxygenated and one olefinic), and eleven quaternary carbons (three olefinic and four carbonyls). The general features of the ^{1}H and ^{13}C NMR data of **2** resembled to those of **1** except for the lack of OCH_3 signals and the obvious downfield shift of C-26. These data revealed that **2** is the 26-COO-demethylated derivative of **1**. The NOEs for **2** (Figure S17) were consistent with those of **1**, suggesting that **2** possess the identical relative configuration with those of **1**. The

experimental ECD spectrum of **2** (Figure S18) was very similar to those of **1** and match well with that calculated for (3*S*, 5*R*, 10*S*, 12*R*, 13*R*, 14*R*, 15*R*, 17*R*)-**1**, indicating their same absolute configurations.

Zebrafish embryos of the AB wild-type strain and TG (VEGFR2: GFP) type strain with fluorescent blood vessels were used to evaluate the cardiovascular effects of compounds **1**–**8** (at concentrations of 20 μg/mL, 50 μg/mL and 100 μg/mL) (Fan et al. 2015). Compounds **1**, **2**, and **4** showed potent promoting angiogenesis activities and **3**, **5**–**6** showed moderate pro-angiogenesis activities in a dose-dependent manner by rescuing PTK787-induced vascular insufficiency in the zebrafish model, while compounds **7** and **8** exhibited lethal effect on the zebrafish embryo (Figure S21). The results suggested that lanostane-type triterpenoids tended to increase the angiogenic activity and could be promising candidates for CVD lead drugs. To the best of our knowledge, this is the first report for cardiovascular effects of lanostane-type triterpenoids in zebrafish.

3. Experimental

3.1. General experimental procedures

(Supplemental material, Experimental section).

3.2. Fungi material

(Supplemental material, Experimental section).

3.3. Extraction and isolation

The powdered fruiting bodies of *G. applanatum* (40 kg) were extracted three times with 95% EtOH in H_2O under reflux at 80 °C. The extract was then suspended in water and partitioned with EtOAc. The combined EtOAc extract (1.3 kg) was subjected to silica gel chromatography (200-300 mesh) using a VLC column, eluting with a stepwise gradient of petroleum ether – CH_2Cl_2 (2:1 and 0:1) and CH_2Cl_2–MeOH (100:1, 90:1, 70:1, 50:1, 30:1, 10:1, 5:1, 1:1, and 0:1) to yield eleven major primary fractions (Fr.1 – Fr.11). Fr. 9 (19.1 g) was further resolved into ten fractions (Fr.9.1–Fr.9.10) by reversed-phase C18 silica column chromatography (CC) (40 × 600 mm) eluting with a stepwise gradient of 1:9 to 1:0 MeOH in H_2O. Fr. 9.5 (65.1 mg) was purified via simi-preparative HPLC with CH_3CN-H_2O (50:50, v/v) as the eluent to give **1** (1.5 mg) and **2** (7.0 mg). Fraction 9.9 (25.0 mg) was subjected to HPLC on ODS (MeOH-H_2O, 60:40, v/v) to yield compound **3** (11.1 mg).

Fr. 7 (53.8 g) was further separated by CC on RP-18 eluting with MeOH-H_2O gradients (1:9 to 1:0) to yield 6 fractions (Frs. 7.1–7.6). Fr. 7.5 (132.2 mg) was recrystallized to give **4** (56.6 mg). The rest of Fr. 7.5 was further subjected to Sephadex LH-20 eluting with MeOH to yield Frs. 7.5.1–7.5.7. Fr. 7.5.7 (65.1 mg) was purified by Sephadex LH-20 eluting with chloroform-methanol (1:1), and then recrystallized to yield **5** (14.6 mg).

Fr. 6 (47.1 g) was purified by CC on silica gel, eluted with petroleum ether-acetic ether (40:1, 30:1, 20:1, 15:1, 10:1, 8:1, 6:1, 4:1, 2:1, 1:1, 0:1) to afford Fr.6.1–6.11. Fr. 6.2 (110.3 mg) was purified by CC on Sephadex LH-20 eluting with chloroform-methanol (1:1) to yield **6** (70.1 mg). Fr. 6.5 (9.1 g) was further resolved into ten fractions (Fr.6.5.1–Fr.6.5.10) by reversed-phase C18 silica CC (40 × 600 mm) eluting with a step-wise gradient of 1:9 to 1:0 MeOH in H_2O. Fraction 6.5.9 was subjected to HPLC on ODS (MeOH-H_2O, 90:10, v/v) to yield compound **7** (30.0 mg). Fr. 6.5.7 (65.1 mg) was purified via simi-preparative HPLC with CH_3OH-H_2O (90:10) as the eluent to give **8** (8.8 mg).

*Ganoderenicfy A (**1**)*: White amorphous powder; [α]25 D= +32.8° (*c* 0.1, MeOH); UV (MeOH) λ_{max}: 248.4 (3.45) nm; ECD (1.13 mmol/L, MeOH) λ_{max} ($\Delta\varepsilon$) 222 (+0.97), 246 (–0.81), 276 (+1.17) nm; IR (KBr) ν_{max} 3379, 2923, 1726, 1626, 1603, 1383, 1161, 1117, 1031, 674 cm^{-1} (Figure S18); HRESIMS *m/z* = 545.3113 ($[M+H]^+$; calcd for $C_{31}H_{45}O_8$: 545.3109); ^1H and ^{13}C NMR data, see Table S1.

*Ganoderenicfy B (**2**)*: White amorphous powder; [α]25 D= +26.9° (*c* 0.1, MeOH); UV (MeOH) λ_{max}: 248.4 (3.40) nm; ECD (1.89 mmol/L, MeOH) λ_{max}($\Delta\varepsilon$) 224 (+0.97), 242 (–1.12), 278 (+1.24) nm; IR (KBr) ν_{max} 3414, 2937, 1713, 1676, 1608, 1456, 1383, 1204, 1115, 1029, 577 cm^{-1} (Figure S18); HRESIMS *m/z* = 531.2968 ($[M+H]^+$; calcd for $C_{30}H_{43}O_8$: 531.2952); ^1H and ^{13}C NMR data, see Table S1.

3.4. Proangiogenic assay

Transgenic zebrafish (Tg(vegfr2:GFP)) expressing enhanced green fluorescent protein (EGFP) in intersomitic vessels (ISV) were used in this study. The zebrafish were maintained under a 14 h light/10 h dark cycle in an automatic circulating tank system with charcoal-filtered tap water to ensure normal spawning. After disinfected, fertilized eggs raised in culture solution in a light-operated incubator at 28.0 °C ± 0.5 °C. Egg membranes were removed from embryos by pronase E solution (1.0 mg/mL) (Shanghai, China) at 24 h post fertilization. A model of vascular insufficiency in zebrafish induced by PTK787 was used to evaluate the effect of compounds **1**-**8** on angiogenesis. Zebrafish embryos were added to 24-well microtiter plates (n = 10/well) treated with 20, 50 and 100 μg/mL of each test compound and 0.2 μg/mL of vatalanib (PTK787, Basel, Switzerland). The positive control was 100 μg/mL ginsenoside Rg1. After 24 h incubation in a light-operated incubator at 28.0 ± 0.5 °C, the number and length of intersegmental vessels (ISV) were captured using a fluorescent microscope (SZX16 Tokyo, Japan) or image acquisition systems (DP2-BSW, Tokyo, Japan) (Fan et al. 2015) (Figure S18). The above assays were repeated eight times with each compound.

4. Conclusion

In conclusion, two new lanostane-type triterpenoids ganoderenicfys A (**1**) and B (**2**) with proangiogenic activities were isolated from the fruiting body of *G. applanatum*. The structures including the relative and absolute configurations were elucidated by NMR, HRESIMS, and quantum chemical ECD calculations. Compounds **1**, **2** and **4** represent the first examples of lanostane-type triterpenoids with the promoting

angiogenesis activities, which suggested that lanostane-type triterpenoids could be promising drug leads for developing new drugs against CVD.

Disclosure statement

No potential conflict of interest was reported by the authors.

Funding

This research was financially by the National Natural Science Foundation of China (42006096), the Shandong Provincial Natural Science Foundation (ZR2020QD098), the Talents of High Level Scientific Research Foundation (Grants 6651120031) of Qingdao Agricultural University and National Key R&D Program of China (Project No. 2018YFD0400200).

References

Benjamin EJ, Muntner P, Alonso A, Bittencourt MS, Callaway CW, Carson AP, Chamberlain AM, Chang AR, Cheng S, Das SR, et al. 2019. Heart disease and stroke statistics-2019 update: a report from the American Heart Association. Circulation. 139(10):e56–e528.

Carmeliet P, Jain RK. 2011. Molecular mechanisms and clinical applications of angiogenesis. Nature. 473 (7347):298–307.

Chatterjee P, Pezzuto JM, Kouzi SA. 1999. Glucosidation of betulinic acid by *cunninghamella* species. J Nat Prod. 62 (5):761–763.

Fan YQ, Li PH, Chao YX, Chen H, Du N, He QX, Liu KC. 2015. Alkaloids with cardiovascular effects from the marine-derived fungus *Penicillium expansum* Y32. Mar Drugs. 13 (10):6489–6504.

Gao SY, Zhang P, Zhang CY, Bao FY, Li H, Chen LX. 2018. Meroterpenoids from ganoderma sinense protect hepatocytes and cardiomyocytes from oxidative stress induced injuries. Fitoterapia. 131:73–79.

Gut P, Reischauer S, Stainier DYR, Arnaout R. 2017. Little fish, big data: zebrafish as a model for cardiovascular and metabolic disease. Physiol Rev. 97 (3):889–938.

Isaka M, Chinthanom P, Sappan M, Supothina S, Vichai V, Danwisetkanjana K, Boonpratuang T, Hyde KD, Choeyklin R. 2017. Antitubercular activity of mycelium-associated *Ganoderma lanostanoids*. J Nat Prod. 80 (5):1361–1369.

Kurusamy S, López-Maderuelo D, Little R, Cadagan D, Savage AM, Ihugba JC, Baggott RR, Rowther FB, Martinez-Martinez S, Gómez-del Arco P, et al. 2017. Selective inhibition of plasma membrane calcium ATPase 4 improves angiogenesis and vascular reperfusion. J Mol Cell Cardiol. 109:38–47.

Luo Q, Yang XH, Cheng YX. 2019. Unprecedented tetranorsesquiterpenoids from *Ganoderma applanatum* mushrooms. Phytochem. Lett. 33:81–83.

Mansoor TA, Hong J, Lee C-O, Bae S-J, Im KS, Jung JH. 2005. Cytotoxic sterol derivatives from a marine sponge *Homaxinella* sp. J Nat Prod. 68 (3):331–336.

Meng J, Yang BX. 2019. Protective effect of *Ganoderma* (Lingzhi) on cardiovascular system. Adv Exp Med Biol. 1182:181–199.

Qin FY, Yan YM, Tu ZC, Cheng YX. 2020. (±) Gancochlearols A and B: cytotoxic and COX-2 inhibitory meroterpenoids from *Ganoderma cochlear*. Nat Prod Res. 34 (16):2269–2275.

Seo HW, Hung TM, Na MK, Jung HJ, Kim JC, Choi JS, Kim JH, Lee HK, Lee IS, Bae KH, et al. 2009. Steroids and triterpenes from the fruit bodies of *Ganoderma lucidum* and their anti-complement activity. Arch Pharm Res. 32 (11):1573–1579.

Sun J, He H, Xie BJ. 2004. Novel antioxidant peptides from fermented mushroom *Ganoderma lucidum*. J Agric Food Chem. 52 (21):6646–6652.

Tung NT, Cuong TD, Hung TM, Lee JH, Woo MH, Choi JS, Kim J, Ryu SH, Min BS. 2013. Inhibitory effect on NO production of triterpenes from the fruiting bodies of *Ganoderma lucidum*. Bioorg Med Chem Lett. 23 (5):1428–1432.

Weng CJ, Fang PS, Chen DH, Chen KD, Yen GC. 2010. Anti-invasive effect of a rare mushroom, *Ganoderma colossum , on human hepatoma cells*. J Agric Food Chem. 58 (13):7657–7663.

Xu Y, Zhu A, Cao F, Liu YF. 2018. Diketopiperazine alkaloids and steroids from a marine-derived *pleosporales* sp. fungus. Chem Nat Compd. 54 (4):818–820.

Yoshikawa K, Nishimura N, Bando S, Arihara S, Matsumura E, Katayama S. 2002. New lanostanoids, elfvingic acids A-H, from the fruit body of *elfvingia applanata*. J Nat Prod. 65 (4): 548–552.

Zhang JJ, Dong Y, Qin FY, Yan YM, Cheng YX. 2019. Meroterpenoids and alkaloids from *Ganoderma austral*. Nat. Prod. Res. 1–7. DOI: 10.1080/14786419.2019.1693565.

Zhou FJ, Nian Y, Yan YM, Gong Y, Luo Q, Zhang Y, Hou B, Zuo ZL, Wang SM, Jiang HH, et al. 2015. Two new classes of T-type calcium channel inhibitors with new chemical scaffolds from *Ganoderma cochlear*. Org Lett. 17(12):3082–3085.